Synthesis of Novel Ferrocene-Benzofuran Hybrids via Palladium- and Copper-Catalyzed Reactions

Nagy, Enikő; Váradi, Márk; Nagymihály, Zoltán; Kollár, László; Kovács, Krisztina; Andreidesz, Kitti; Gömöry, Ágnes; Tumanov, Nikolay; Wouters, Johan; Skoda-Földes, Rita

Published in:
Inorganics

DOI:
10.3390/inorganics10110205

Publication date:
2022

inorganics

MDPI

Article

Synthesis of Novel Ferrocene-Benzofuran Hybrids via Palladium- and Copper-Catalyzed Reactions

Enikő Nagy [1], Márk Váradi [1], Zoltán Nagymihály [2], László Kollár [2,3], Krisztina Kovács [4], Kitti Andreidesz [4], Ágnes Gömöry [5], Nikolay Tumanov [6], Johan Wouters [6] and Rita Skoda-Földes [1,*]

1 Research Group of Organic Synthesis and Catalysis, Center of Natural Sciences, University of Pannonia, Egyetem u. 10, H-8200 Veszprém, Hungary
2 Department of Inorganic Chemistry and ELKH-PTE Research Group for Selective Chemical Syntheses, University of Pécs, Ifjúság u. 6, H-7624 Pécs, Hungary
3 Szentágothai Research Centre, H-7624 Pécs, Hungary
4 Department of Biochemistry and Medical Chemistry, Medical School, University of Pécs, Szigeti út 12, H-7624 Pécs, Hungary
5 Research Centre for Natural Science, Eötvös Loránd Research Network, Magyar Tudósok Körútja 2, H-1117 Budapest, Hungary
6 Department of Chemistry, Namur Institute of Structured Matter (NISM), University of Namur, Rue de Bruxelles 61, B-5000 Namur, Belgium
* Correspondence: skodane.foldes.rita@mk.uni-pannon.hu

Abstract: The combination of the ferrocene skeleton with pharmacophores often leads to molecules with interesting biological properties. Five ferrocene-benzofuran hybrids of different structures were synthesized by transition metal catalyzed reactions. The efficiency of both homogeneous and heterogeneous catalytic methods was tested. The products were characterized using ^{1}H, ^{13}C NMR and FTIR spectroscopy, HRMS and cyclic voltammetry. The structure of one of the new compounds was also proved with X-ray crystallography. The new hybrids showed moderate cytotoxicity on MCF-7 and MDA-MB-231 cell lines. It is remarkable that the less curable MDA-MB-231 cell line was more sensitive to treatment with three ferrocene derivatives.

Keywords: ferrocene; benzofuran; homogeneous catalysis; heterogeneous catalysis; cytotoxicity

check for updates

Citation: Nagy, E.; Váradi, M.; Nagymihály, Z.; Kollár, L.; Kovács, K.; Andreidesz, K.; Gömöry, Á.; Tumanov, N.; Wouters, J.; Skoda-Földes, R. Synthesis of Novel Ferrocene-Benzofuran Hybrids via Palladium- and Copper-Catalyzed Reactions. *Inorganics* **2022**, *10*, 205. https://doi.org/10.3390/inorganics10110205

Academic Editor: Lubov Snegur

Received: 6 October 2022
Accepted: 7 November 2022
Published: 11 November 2022

1. Introduction

Benzofurans possess diverse biological properties, which makes them an attractive motif for further modifications. Depending on the type, number and position of functional groups, benzofuran derivatives were shown to serve as radical scavengers to trap reactive oxygen species (ROS) [1] and to exhibit anti-microbial [2–4], anti-inflammatory [4] and anticancer [5] activities. The benzofuran core was also found to be a promising scaffold to develop new drugs to treat Alzheimer's disease [6]. Various clinically approved drugs are based on this pharmacophore such as antidepressants citalopram [7] and vilazodone [8] or amiodaron and dronedarone used to cure patients with atrial fibrillation [9].

The 1,2,3-triazole scaffold is also considered to be a significant fragment in medicinal chemistry. Due to its unique features like participation in hydrogen bonding and dipole-dipole interactions, 1,2,3-triazole-containing compounds are popular in drug discovery [10,11]. They have been shown to possess antibacterial [12], antitumor [13,14], antifungal [15], antimicrobial [16] and anti-HIV activities [17]. Moreover, these five-membered rings can be generated with copper-catalyzed cycloadditions selectively and under conditions suitable for biological systems [18]. These properties render them useful linkers to produce hybrid molecules of various scaffolds.

Since the success of cisplatin in cancer therapy, the importance of transitionmetal-containing molecules in medicine is constantly increasing [19–21]. Among versatile biologically active metallocenes, ferrocene has many favorable features, e.g., non-toxicity, excellent

redox properties, stability and good solubility in organic solvents. Ferrocene is a promising building block due to the diverse biological activity of ferrocenyl compounds such as cytotoxic, antitumor, antimalarial, antifungal and DNA-cleaving activity [22,23]. Introduction of ferrocene has a strong influence on pharmacological activities of drug molecules; a prominent example is the chemoterapeutic agent tamoxifen and its functionalized form, ferrocifen [24], as well as the antimalarial agent ferroquine [25].

The significance of the three motifs and their derivatives justifies the search for new synthetic methodologies resulting in benzofuran derivatives including novel ferrocene-triazole-benzofuran and ferrocene-benzofuran hybrids.

The literature describes only a few examples for ferrocenyl- or triazolyl-benzofurans. Torres et al. reported a homogeneous, $PdCl_2(PPh_3)_2$ catalyzed coupling-annulation reaction resulting in 2-ferrocenyl-2-benzo[*b*]furan [26]. Zhao et al. introduced the ferrocenyl group to natural compounds with the benzofuran core which led to an increase in their efficiency as antioxidants [27]. The enhanced antibacterial activity of ferrocenyl aurones compared to ferrocenyl chalcones suggested the key role of the benzofuran core [28]. Zhuoma et al. developed a synthetic method for 2-ferrocenoyl-benzofuran derivatives using the Rap–Stoermer reaction, however the biological effect was not investigated in these cases [29,30]. Benzofuran-based 1,2,3-triazoles were found to exhibit antifungal [31], antimicrobial [32] and tubulin polymerization inhibitory [33] activity. The triazol ring was formed by copper-catalyzed cycloaddition reactions in each example.

In the present research, palladium-catalyzed coupling and carbonylation reactions were applied to synthesize benzofuran-ferrocene hybrids and to introduce reactive alkynyl moieties that make further functionalization of the skeleton possible. The 1,2,3-triazole motifs were synthesized via copper-catalyzed cycloaddition reactions.

Recently, heterogeneous alternatives to transition metal catalysts have attracted a considerable interest from researchers due to advantages such as easier separation and recyclability [34–37]. While homogeneous catalysis has become a versatile methodology in the production of pharmaceutical intermediates [38,39], fine chemicals, agrochemicals etc., with complicated structures, the application of heterogeneous catalysts is restricted to simple derivatives in most cases [27,34,36,40]. In the present report, beside homogeneous reactions, the applicability of supported catalysts in the synthesis of novel ferrocene-benzofuran and ferrocene-triazole-benzofuran hybrids was studied.

2. Results and Discussion

2.1. Preparation of the Heterogeneous Catalysts

Silica, modified using a pyridinium-based ionic liquid, was used as the support of the heterogeneous palladium catalyst. A permanent linkage between the pyridinium moiety and surface hydroxyl groups was formed by reacting 3-(triethoxysilyl) propyl-pyridinium iodide with silica (Scheme 1). The heterogeneous catalyst was obtained using $Pd_2(dba)_3$ $CHCl_3$ as the palladium precursor. The palladium content of the catalyst proved to be in the range of 0.70–0.72%, based on the results of ICP-AES measurements. FT-IR, ^{13}C CP MAS NMR, and TEM techniques were used to characterize the catalyst and the data has been reported before [41]. It had been shown to be highly active, selective and reusable in aminocarbonylation as well as Sonogashira and Suzuki reactions. Amides and ketoamides with simple structures or even pharmacologically active molecules as well as diverse benzofuran derivatives were efficiently synthesized in the presence of this Pd-pyridinium-SILP [41,42].

The heterogeneous copper catalyst was prepared using the deposition of copper on a polymer-modified silica support (Scheme 2). The polymerization of 1-methyl-3-(4-vinylbenzyl) imidazolium chloride was carried out in the presence of silica gel to prepare the inorganic/organic hybrid support and copper was immobilized on the surface in the presence of *t*BuOK using CuI as the precursor. According to ICP-AES measurements, the copper content of the catalyst was in the range of 2.9–3.1%. In the former research the heterogeneous catalyst was characterized using ^{13}C CP MAS NMR, FT-IR spectroscopies [43]. It has proved to be highly active in the reaction of simple alkynes and azides, however in the presence of

azidomethylferrocene its activity has been shown to be strongly dependent on the structure of the alkyne. The product 1,2,3-triazoles can be obtained with good yields from the reaction of propargylic acetate (93%) or methyl propiolate (87%), while cycloaddition of ethynylestradiol led to only 24% of the corresponding product under identical conditions.

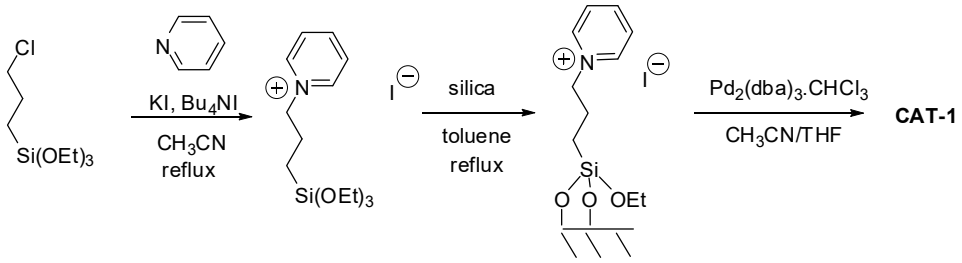

Scheme 1. Preparation of the heterogeneous Pd-catalyst **CAT-1**.

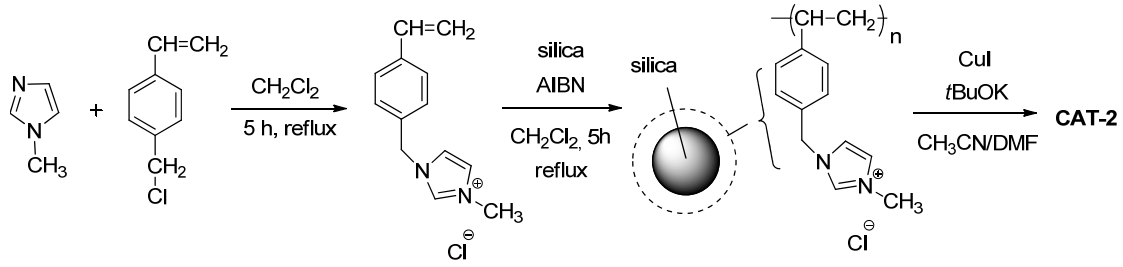

Scheme 2. Preparation of the heterogeneous Cu-catalyst **CAT-2**.

2.2. Synthesis of Ferrocene-Triazole-Benzofuran Hybrides

Two different two-step reactions resulting in ferrocene-triazole-benzofuran hybrids were studied. First an ethynyl moiety was attached to the benzofuran core, either via an aminocarbonylation reaction (Scheme 3) or via a Sonogashira coupling (Scheme 4). Then the introduction of ferrocene was enabled by the use of ferrocenylmethylazide as the reaction partner in azide-alkyne cycloadditions.

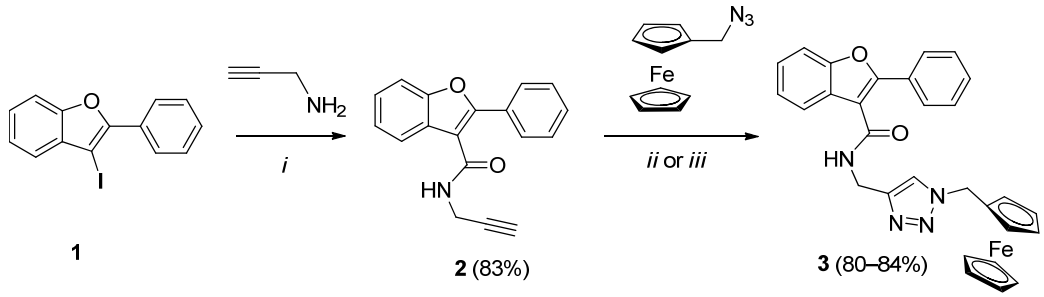

Scheme 3. Synthesis of benzofuran-triazole-ferrocene hybrid **3** (Reaction conditions: (*i*) **CAT-1** (1.4 mol% Pd), 20 bar CO, DMF, Et_3N, 100 °C, 7 h; (*ii*) $CuSO_4 \cdot 5H_2O$ (15 mol%), Na-ascorbate, CH_2Cl_2/H_2O, rt, 7 h; (*iii*) **CAT-2** (10 mol% Cu), CH_2Cl_2, rt, 24 h).

In the first step, propargylamine was used as a nucleophilic reagent to provide a free ethynyl-group in the product. According to previous studies, the optimal conditions for aminocarbonylation reactions with the heterogeneous catalyst involve the application of DMF/Et_3N solvent/base system at 100 °C under CO pressure [41], so the present experiments were carried out accordingly. To achieve full conversion of 3-iodo-2-phenylbenzofuran (**1**) to product **2**, the presence of five equivalents of propargylamine was required. The amide intermediate (**2**) was isolated with an 83% yield. (The methodology for chromatographic separation was not optimized). The catalyst could be reused in eight further runs without noticeable change in its activity (total conversion under the same reaction conditions). Pd

loss was 5% of the original amount, which dropped to 2% in the 9th run. The next step of the reaction route was an azide-alkyne cycloaddition, leading to the selective formation of triazole **3** in the presence of copper catalysts. The application of both homogeneous and heterogeneous conditions led to full conversion of substrates and provided the target molecule **3** with 80–84% isolated yield. The reaction conditions have been chosen based on the previous results of our research group [43,44]. The $CuSO_4$/Na-ascorbate system in dichloromethane/water solvent mixture proved to be suitable for homogeneous reactions while the heterogeneous catalyst was applied in dichloromethane in the absence of any further additive.

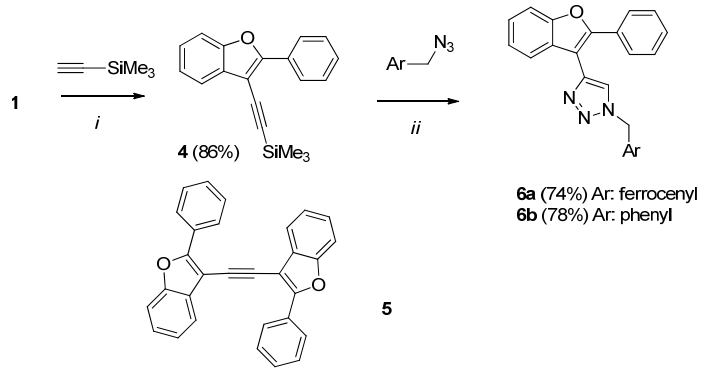

Scheme 4. Synthesis of benzofuran-triazole-ferrocene hybrid **6a** and its Ph analogue **6b** (Reaction conditions: (*i*) $PdCl_2(PPh_3)_2$ (4 mol%), CuI (4 mol%), Et_3N, rt, 2 h, (*ii*) $CuSO_4 \cdot 5H_2O$ (15 mol%), Na-ascorbate, TBAF, CH_2Cl_2/H_2O, rt, 7 h).

Another multi-step reaction route resulting in the triazolyl-functionalized benzofuran **6a** was also studied (Scheme 4). At first the conditions of the palladium-catalyzed Sonogashira reaction of the iodo-containing benzofuran derivative **1** and ethynyltrimethylsilane were optimized (Table 1). Only a low conversion of iodobenzofuran **1** could be observed in DMF solvent even at 80–100 °C (entries 1,2) using Et_3N as the base. The application of an inorganic base (KOAc) promoted in situ deprotection of the alkyne **4** especially at 100 °C, which was followed by a further Sonogashira reaction leading to the dimeric structure (**5**) (entries 3,4). (In situ deprotection of trimethylsilylacetylenes followed by Sonogashira coupling is a widely used method for the synthesis of disubstituted acetylenes. Deprotection was reported to be achieved by the addition of KOH, fluorides [45] or K_2CO_3 [46]). A significant increase in the conversion and selective formation of product **4** was observed when triethylamine was used as the base and solvent (entry 6) at room temperature. At the same time, good results were achieved only after prolonged interaction or with the application of a homogeneous catalyst ($PdCl_2(PPh_3)_2$) (entry 7). The alkynyl derivative **4** was purified by column chromatography and was obtained in 50% and 86% isolated yields via the heterogeneous (entry 6) and homogeneous coupling reactions (entry 7), respectively.

Table 1. Optimization of the Sonogashira coupling of iodobenzofuran **1** and ethynyltrimethylsilane.

Entry	Catalyst	Solvent	Base	Temp. (°C)	R.Time (h)	Conv. (%) [c]	Ratio of 4/5 [c]
1 [a]	**CAT-1**	DMF	Et_3N	80	2	5	5/0
2 [a]	**CAT-1**	DMF	Et_3N	100	2	7	7/0
3 [a]	**CAT-1**	DMF	KOAc	80	2	20	4/16
4 [a]	**CAT-1**	DMF	KOAc	100	2	100	0/100
5 [b]	**CAT-1**	Et_3N	Et_3N	rt	2	20	20/0
6 [a]	**CAT-1**	Et_3N	Et_3N	rt	24	60	60/0
7 [a]	$PdCl_2(PPh_3)_2$	Et_3N	Et_3N	rt	2	100	100/0

[a] Reaction conditions: catalyst (5 μmol Pd), CuI (5 μmol), **1** (0.1 mmol), ethynyltrimethylsilane (0.2 mmol), base (0.2 mmol) DMF (2 mL). [b] Reaction conditions: catalyst (4 μmol Pd), CuI (4 μmol), **1** (0.1 mmol), ethynyltrimethylsilane (0.2 mmol), Et_3N (215 μL). [c] Determined by GC.

Based on some examples from the literature [47–49], the formation of the triazol ring via azide-alkyne cycloaddition was enabled using the in situ deprotection of the alkyne moiety. After the removal of the excess of triethylamine and ethynyltrimethylsilane in vacuum, the reaction mixture was used directly in the cycloaddition. As TBAF seemed to be a promising desilylation agent, it was combined with the formerly used $CuSO_4$/Na-ascorbate system in a dichloromethane/water solvent mixture. The one-pot deprotection and cycloaddition was carried out successfully, resulting in the desired product **6a** yielding 74%, starting from iodobenzofuran **1**. In order to compare biological activities of the ferrocene hybrid **6a** and a compound without the ferrocenyl moiety, the phenyl derivative **6b** was produced in a similar fashion.

2.3. Synthesis of Ferrocene-Benzofuran Hybrides

The ferrocene and benzofuran cores were also attached directly via aminocarbonylation (Scheme 5) and Sonogashira reactions (Scheme 6) to obtain novel hybrids. Based on the former results related to aminocarbonylations [41], the heterogeneous catalyst **CAT-1** was used to functionalize 3-iodo-2-phenylbenzofuran (**1**) with aminomethylferrocene. The formerly applied conditions (DMF, Et_3N and 100 °C) led to a full conversion of substrate **1** even using the amine reagent in an equimolar amount (Scheme 5). However, in this case, hydrodehalogenation of **1**, leading to benzofuran **8** was observed as a side reaction and product **7** was isolated with a yield of 61%.

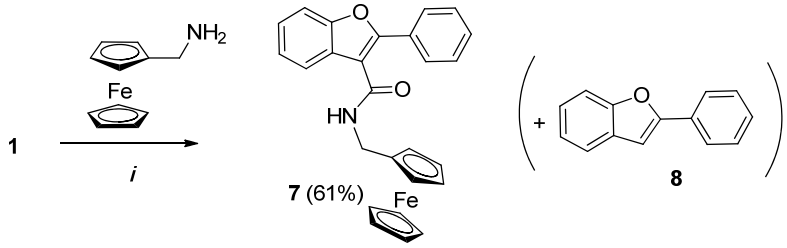

Scheme 5. Synthesis of ferrocene-benzofuran hybrid **7** via aminocarbonylation (Reaction conditions: (*i*) **CAT-1** (1.4 mol% Pd), 20 bar CO, DMF, Et_3N, 100 °C, 7 h).

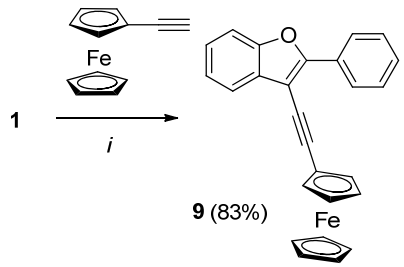

Scheme 6. Synthesis of ferrocene-benzofuran hybrid **9** via Sonogashira coupling. (Reaction conditions: (*i*) **CAT-1** (2.8 mol% Pd), CuI (2.8 mol%), DMF, KOAc, 100 °C, 3 h).

The efficiency of the heterogeneous palladium catalyst **CAT-1** was also investigated in the Sonogashira reaction of ethynylferrocene and 2-phenyl-3-iodobenzofuran (**1**) (Scheme 6). Previous results [42] showed that DMF/KOAc solvent/base system could be efficiently applied in the Sonogashira reaction of benzofuran derivative **1**. Similar to previous findings, full conversion was achieved, even using a catalyst/substrate ratio of 2.8 mol%, although in a more prolonged reaction (3 h) compared to the coupling carried out with a catalyst/substrate ratio of 5 mol% (1 h). Hybrid **9** was obtained with a high isolated yield (83%) after purification. The reuse of the catalyst resulted in a somewhat lower yield of product **9** (73%). According to an ICP-AES measurement, 6% of the original amount of the Pd catalyst was lost in the first cycle.

The benzofuran derivative **11** was synthesized using a two-step reaction sequence starting with Sonogashira coupling and followed by an aminocarbonylation reaction (Scheme 7).

In the first step 4-ethynylaniline was used as the reagent to introduce the amine functionality. Intermediate **10** was produced with a high conversion (94%) and a good yield (83%) in the presence of catalyst **CAT-1,** according to our previous report [42]. The same heterogeneous catalyst has proved to be efficient in the second, carbonylation step starting from iodoferrocene and benzofuran **10**. The product (**11**) was obtained in excellent yield (98%).

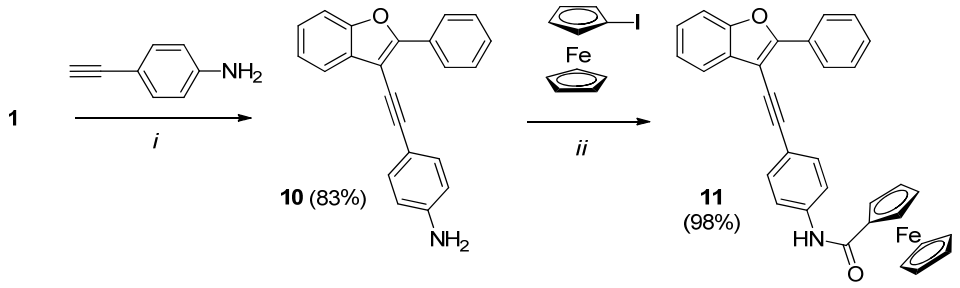

Scheme 7. Synthesis of ferrocene-benzofuran hybrid **11** via a Sonogashira coupling-aminocabonylation reaction sequence (Reaction conditions: (*i*) **CAT-1** (2.8 mol% Pd), DMF, KOAc, 100 °C, 10 h; (*ii*) **CAT-1** (1.4 mol% Pd), 20 bar CO, DMF, Et_3N, 100 °C, 7 h).

All the ferrocene-benzofuran hybrids were characterized using ^1H, $^{13}C\{^1H\}$ NMR, IR and HRMS measurements. In the case of compound **9**, crystals suitable for single-crystal X-ray diffraction were grown and analyzed. The results showed that the cyclopentadienyl rings of the ferrocenyl moiety are perpendicular to the plane of the benzofuran core (Figure 1).

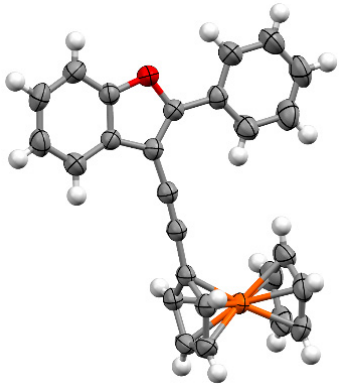

Figure 1. Molecular structure of compound **9**. Thermal ellipsoids are shown at 50% probability level.

2.4. Electrochemistry

Cyclic voltammetry measurements were carried out to investigate the electrochemical behavior of the novel hybrid molecules. Cyclic voltammograms showed reproducible and well-defined anodic and cathodic peaks. The hybrids can be oxidized at higher anodic potentials than ferrocene (Table 2, Figure 2) due to the electron withdrawing substituents attached to the cyclopentadienyl ring. (Different peak currents are due to the different diffusion coefficients (*D*) of the ferrocene derivatives. The *D* values were determined from the slope of a plot constructed by measuring the peak currents as a function of the square root of the polarization rate.) The two carboxamides **7** and **11** showed the lowest and the highest $E_{1/2}$ values, respectively, due to the presence of the aminomethyl- and carboxamide functionalities. Because of the small difference in the redox potentials of some of the hybrids, especially **7**, and ferrocene, redox potentials relative to ferrocene were determined using SWV measurements of solutions of benzofuran hybrids containing ferrocene as an internal standard (see Supplementary Materials). The relative peak potentials (E_{rel}) were calculated by fitting a Gaussian curve, as described in Section 3.4.

Table 2. Diffusion coefficients (D), half wave potentials ($E_{1/2}$) and redox potentials relative to ferrocene (E_{rel}) of ferrocene–benzofuran hybrids [a].

Compound	D (cm^2 s^{-1}) × 10^6	$E_{1/2}$ (mV) [b]	E_{rel} (mV) [c]
Fc	11.70	503	0
3	4.22	624	159.4
6a	4.30	618	169.0
7	8.34	553	121.1
9	2.05	645	164.2
11	3.62	698	224.5

[a] Working electrode: glassy carbon, reference electrode: Ag/AgCl (H_2O), auxiliary electrode: Pt wire, concentration: 2.5 × 10^{-3} M in CH_2Cl_2, supporting electrolyte: 0.1 M *n*-Bu_4NPF_6; [b] scan rate 50 mV/s; [c] $E_{rel} = E - E$(Fc), determined by SWV measurements using Fc (1.25 × 10^{-3} M) as internal standard.

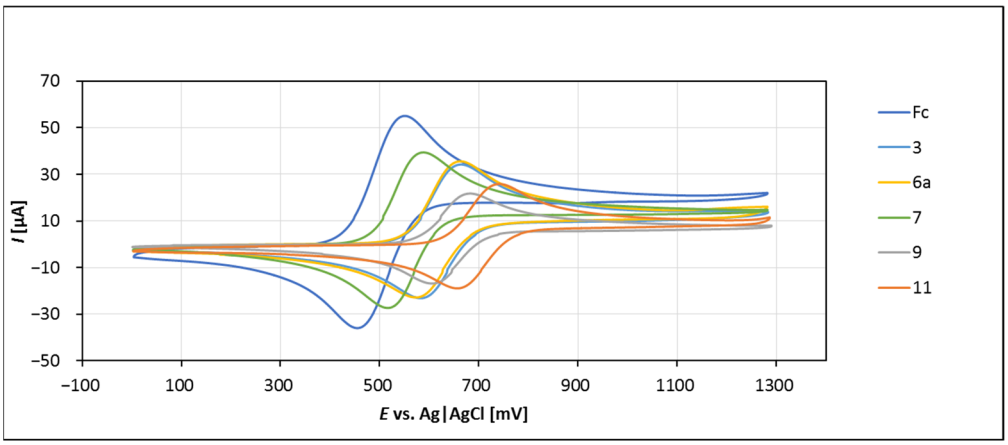

Figure 2. Cyclic voltammograms of ferrocene-benzofuran hybrids and ferrocene (Fc) (working electrode: glassy carbon, reference electrode: Ag/AgCl (H_2O), auxiliary electrode: Pt wire, concentration: 2.5 × 10^{-3} M in CH_2Cl_2, supporting electrolyte: 0.1 M *n*-Bu_4NPF_6, scan rate: 50 mV/s).

2.5. Biological Activity of Ferrocenyl Derivatives

The toxicity of ferrocene-benzofuran derivatives **3**, **6a**, **7** and **9** were tested on MCF7 (Figure 3) and MDA-MB-231 (Figure 4) cell lines. (The Pd content of the samples after chromatographic separation was checked for compound **7** (14 ppm) and compound **9** (42 ppm) by ICP-AES). The sulforhodamine B (SRB) assay was used to examine cell viability. The SRB assay measures protein content, and this methodology is regarded as more proportional to the cell count than to metabolic activity. Results obtained with samples of biologically relevant concentrations (10 μM and 25 μM) are shown in Figures 3 and 4; the data obtained with solutions of higher concentrations are included in the supporting information. (For comparison, the results obtained with compound **6b**, the phenyl analogue of **6a**, are also included). Compound **9** not containing a carboxamido- or triazolyl group only affected the cell lines at higher concentrations. Hybrids **3**, **6a**, and **7** showed higher effectiveness in toxicity measurements. A significant decrease in cell survival could be detected even in the 10 μM concentrations of compounds **3**, **6a**, and **7** after 48 h treatments. It should be mentioned that MDA-MB-231 cells which are considered to be more aggressive and less curable, exhibited higher sensitivity to **3**, **6a**, and **7** treatments.

The phenyl analogue **6b** exerted a small effect on MCF7 cells. Interestingly, it showed greater toxicity to MDA-MB-231 cells than the ferrocenyl compound **6a** in low concentrations ($c \leq 10$ μM). However, in contrast to compound **6a**, cell survival could not be reduced by a further increase in the concentration of **6b** ($c \geq 25$ μM).

Although the cytotoxicity of ferrocene derivatives is often attributed to their oxidation to ferrocenium derivatives (see previous studies [50]), no correlation can be observed between the redox potentials and cytotoxicity of the ferrocene-benzofuran hybrids.

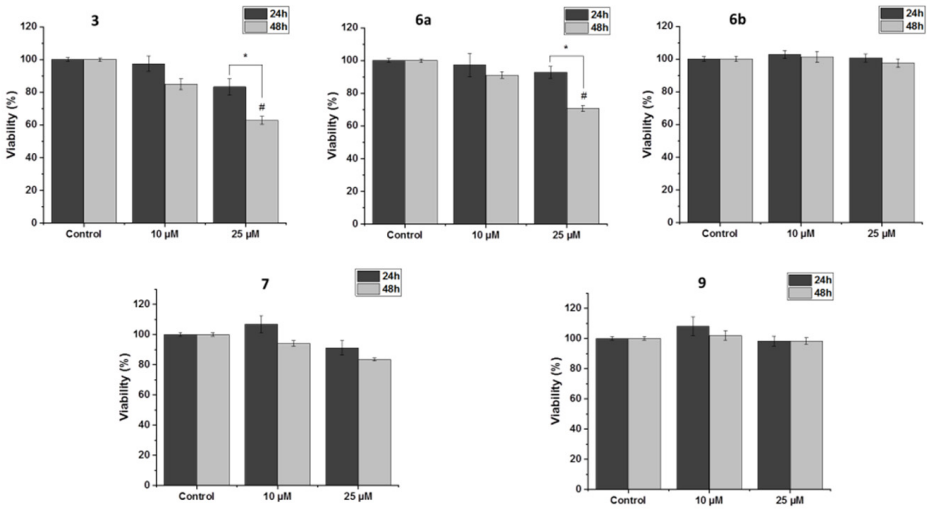

Figure 3. The effects of compounds **3**, **6a**, **6b**, **7** and **9** on the viability of MCF7 cells, evaluated by MTT assay. Cells were treated with 10 μM and 25 μM for 24 h or 48 h. Data are shown as mean ± SEM of at least three separate experiments. * $p < 0.05$ compared with the untreated cells. #: $p < 0.05$ compared with the cells treated with 10 μM solutions.

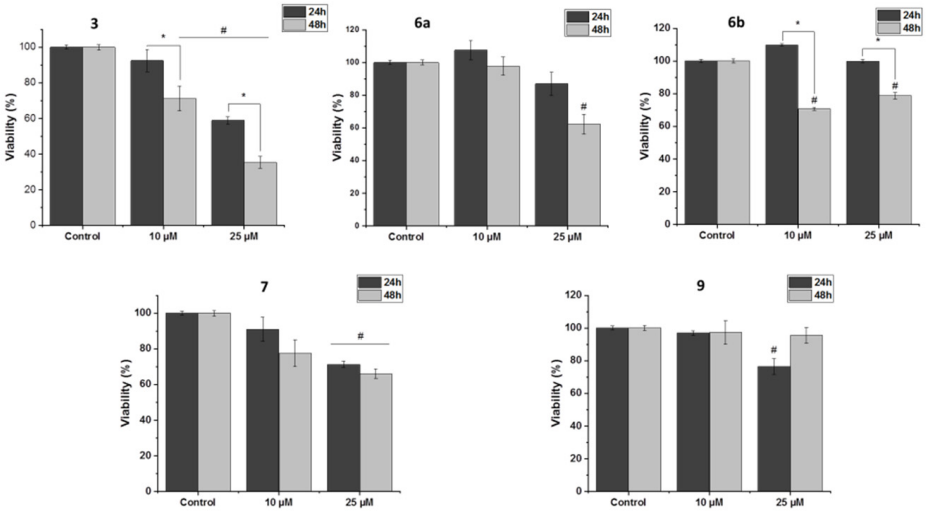

Figure 4. The effects of compounds **3**, **6a**, **6b**, **7** and **9** on the viability of MDA-MB-231 cells, evaluated by MTT assay. Cells were treated with 10 μM and 25 μM for 24 h or 48 h. Data are shown as mean ± SEM of at least three separate experiments. * $p < 0.05$ compared with the untreated cells. #: $p < 0.05$ compared with the cells treated with 10 μM solutions.

3. Materials and Methods

3.1. General Information

Gas chromatography (Hewlett Packard 5890, SPB-1 column) and GC-MS (Hewlett Packard 5971A GC-MSD, DB-5MS column) were used to analyze reaction mixtures. ^{1}H and ^{13}C{^{1}H} NMR spectra were acquired on a Bruker Avance 400 spectrometer in $CDCl_3$ and DMSO-d_6 at 400.13 MHz and 100.62 MHz, respectively. FT-IR spectra of samples (in KBr pellets) were obtained on a Thermo Nicolet Avatar 330 FT-IR and Shimadzu IRAffinity-1S FT-IR spectrometer. A Q-TOF Premier mass spectrometer (Waters Corporation, Milford, MA, USA) in positive electrospray ionization mode was used for the acquisition of HRMS data.

The preparation of the heterogeneous palladium [41] and copper catalyst [43], as well as synthetic methodology to prepare 3-iodo-2-phenylbenzofuran (**1**) [42], azidomethylferrocene [51] and ferrocenylmethylamine [52] have been described before. All other reactants were purchased from commercial sources and were used as received.

3.2. Synthetic Procedures

3.2.1. Synthesis of 2-Phenyl-*N*-(prop-2-yn-1-yl)benzofuran-3-carboxamide (**2**)

The catalyst **CAT-1** (containing 1.4 μmol Pd), 3-iodo-2-phenylbenzofuran (**1**) (0.1 mmol, 32 mg), propargylamine (0.5 mmol, 27.5 mg, 32 μL), triethylamine (0.15 mmol, 15 mg, 20 μL) and DMF (1 mL) were placed in a stainless-steel autoclave. It was charged with carbon monoxide (20 bar) and heated while stirring in an oil bath at 100 °C for 7 h. The catalyst was allowed to settle at room temperature and then the liquid phase was separated with a syringe. The reaction mixture was analyzed by TLC and gas chromatography. After the evaporation of the solvent, the crude product was purified by column chromatography (silica, eluent: toluene/ethyl acetate 10:1) to produce **2** as a white solid in 83% yield.

^{1}H NMR (400.13 MHz, $CDCl_3$) δ: 7.86–7.95 (m, 3H, 4-H and 2′,6′-H), 7.45–7.55 (m, 4H, 7-H and 3′,4′,5′-H), 7.28–7.39 (m, 2H, 5,6-H), 6.08 (s, 1H, NH), 4.24 (dd, J = 2.5 Hz, 5.4 Hz, 2H, CH_2), 2.26 (t, J = 2.5 Hz, 1H, ≡CH).

^{13}C{^{1}H} NMR (100.62 MHz, $CDCl_3$) δ: 163.60 (C=O), 155.36 (2-C), 153.92 (7a-C), 130.22 (4′-C), 129.29 (3-C), 128.99 (2C, 3′,5′-C), 128.53 (2C, 2′,6′-C), 127.58 (1′-C), 125.49 (5-C), 123.98 (6-C), 121.24 (4-C), 112.16 (3a-C), 111.36 (7-C), 79.14 (CH_2-$\underline{C}$≡CH), 71.99 (C≡$\underline{C}$H), 29.38 (CH_2).

FT-IR (KBr, cm^{-1}): 3301; 3265; 3060; 2932; 1646; 1523; 1454; 1446; 1343; 1245; 1127; 739; 694.

MS (*m*/*z*/rel.int.): 275[M$^+$]/70; 246/41; 231/16; 222/22; 221/100; 194/27; 165/81; 164/19; 163/16; 139/15; 39/34.

3.2.2. Synthesis of *N*-((1-Ferrocenylmethyl-1*H*-1,2,3-triazol-4-yl)methyl)-2-phenylbenzofuran-3-carboxamide (**3**)

Under homogeneous conditions: A mixture of $CuSO_4 \cdot 5H_2O$ (0.015 mmol, 4 mg), Na-ascorbate (0.038 mmol, 8 mg), 2-phenyl-*N*-(prop-2-yn-1-yl)benzofuran-3-carboxamide (**2**) (0.1 mmol, 27.5 mg), ferrocenylmethylazide (0.1 mmol, 24.1 mg), dichloromethane (1 mL) and distilled water (1 mL) was stirred under an argon atmosphere at room temperature for 7 h. The conversion was followed by TLC and gas chromatography. Then, dichloromethane (3 mL) was added to the reaction mixture. The combined organic phase was washed with water (3 × 2 mL), dried over Na_2SO_4 and concentrated. The product was purified using column chromatography (silica, eluent: toluene/acetone 4:1) to obtain compound **3** as a yellow solid in 84% yield.

Under heterogeneous conditions: A mixture of **CAT-2** (containing 0.01 mmol Cu), 2-phenyl-*N*-(prop-2-yn-1-yl)benzofuran-3-carboxamide (**2**) (0.1 mmol, 27.5 mg), ferrocenylmethylazide (0.1 mmol, 24.1 mg) and dichloromethane (1 mL) was stirred under an argon atmosphere at room temperature for 24 h. The conversion was followed by TLC and gas chromatography. Dichloromethane (3 mL) was added, and a liquid phase was separated with a syringe. Then the catalyst was washed three times with 3 mL dichloromethane. The solutions were combined and concentrated under vacuum. The product was purified using column chromatography (silica, eluent: toluene/acetone 4:1) to obtain compound **3** as a yellow solid in 80% yield.

^{1}H NMR (400.13 MHz, DMSO-d_6) δ: 9.04 (t, J = 5.8 Hz, 1H, NH), 7.98 (s, 1H, CH of triazole ring), 7.79–7.85 (m, 2H, 2′,6′-H), 7.64–7.68 (m, 1H, 7-H), 7.59–7.64 (m, 1H 4-H), 7.36–7.46 (m, 4H, 6-H and 3′,4′,5′-H), 7.28–7.34 (m, 1H, 5-H), 5.34 (s, 2H, N-$\underline{C}H_2$-Cp), 4.54 (d, J = 5.8 Hz, 2H, NH-$\underline{C}H_2$-triazole), 4.35 (t, J = 1.8 Hz, 2H, 2,5-C of substituted Cp ring), 4.21 (s, 5H, unsubstituted Cp ring), 4.19 (t, J = 1.8 Hz, 2H, 3,4-C of substituted Cp ring).

^{13}C{^{1}H} NMR (100.62 MHz, DMSO-d_6) δ: 163.08 (C=O), 152.81 (7a-C), 152.24 (2-C), 144.31 (4-C of triazole ring), 129.46 (4′-C), 128.97 (1′-C), 128.78 (2C, 3′,5′-C), 127.53 (3-C), 126.72 (2C, 2′,6′-C), 125.39 (6-C), 123.55 (5-C), 122.43 (5-C of triazole ring), 120.60 (4-C), 113.64 (3a-C), 111.19 (7-C), 82.44 (1-C of substituted Cp ring), 68.69 (2C, 2,5-C of substituted Cp ring), 68.67 (5C, unsubstituted Cp ring), 68.35 (2C, 3,4-C of substituted Cp ring), 48.90 (N-$\underline{C}H_2$-Cp), 34.57 (NH-$\underline{C}H_2$-triazole).

FT-IR (KBr, cm^{-1}): 3412; 3391; 3121; 3101; 3048; 1650; 1511; 1495; 1454; 1442; 1230; 1119; 1103; 1046; 751.

HRMS: *m*/*z* calcd for $C_{29}H_{24}FeN_4O_2$ [M]$^+$: 516.1249; found: 516.1236.

3.2.3. Synthesis of Trimethyl((2-phenylbenzofuran-3-yl)ethynyl)silane (**4**)

In DMF: The catalyst **CAT-1** (containing 5 μmol Pd), CuI (5 μmol, 1 mg), 3-iodo-2-phenylbenzofuran (**1**) (0.1 mmol, 32 mg), ethynyltrimethylsilane (0.2 mmol, 19.6 mg, 29 μL), base (0.2 mmol) and DMF (2 mL) were heated while stirring under an argon atmosphere. The conversion was followed by TLC and gas chromatography.

In Et_3N: The catalyst **CAT-1** (containing 4 μmol Pd) or $PdCl_2(PPh_3)_2$ (4 μmol, 3 mg), CuI (4 μmol, 0.8 mg), 3-iodo-2-phenylbenzofuran (**1**) (0.1 mmol, 32 mg), ethynyltrimethylsilane (0.2 mmol, 19.6 mg, 29 μL), triethylamine (215 μL) were stirred under inert conditions at room temperature. The conversion was followed by TLC and gas chromatography. (In the heterogeneous reaction, the solution phase was separated with a syringe. Then the catalyst was washed with 2 mL dichloromethane). The combined organic phases were filtered through celite and concentrated under a vacuum. The crude product was used without further purification in the next step, or purified using column chromatography (silica, eluent: hexane/dichloromethane 80:1) to produce compound **4** as a white solid in 50% yield (in the presence of **CAT-1**) or in 86% yield (in the presence of $PdCl_2(PPh_3)_2$).

Analytical data of compound **4** corresponded well to those reported before [42].

Side product 1,2-*bis*(2-phenylbenzofuran-3-yl)ethyne (**5**) was characterized using GC-MS. MS (*m*/*z*/rel.int.): 410[M^+]/100; 379/11; 205/8; 175/11; 77/7.

3.2.4. Synthesis of 1-Ferrocenylmethyl-4-(2-phenylbenzofuran-3-yl)-1*H*-1,2,3-triazole (**6a**) and 1-Phenylmethyl-4-(2-phenylbenzofuran-3-yl)-1*H*-1,2,3-triazole (**6b**)

A mixture of $CuSO_4 \cdot 5H_2O$ (0.015 mmol, 4 mg), Na-ascorbate (0.038 mmol, 8 mg), the crude product of the previous step, ferrocenylmethylazide or benzylazide (0.2 mmol), TBAF (0.2 mmol, 52.3 mg), dichloromethane (1 mL) and distilled water (1 mL) was stirred under an argon atmosphere at room temperature for 7 h. The conversion was followed by TLC and gas chromatography. Then, dichloromethane (3 mL) was added to the reaction mixture. The combined organic phases were washed with water (3 × 2 mL), dried over Na_2SO_4 and concentrated. The crude products were purified using column chromatography (silica, eluent: toluene/ethyl acetate 15:1) to obtain the compound **6a** as a dark yellow solid in 74% yield and **6b** as a white solid in 78% yield.

6a: ^{1}H NMR (400.13 MHz, $CDCl_3$) δ: 7.85–7.88 (m, 1H, 4-H), 7.80–7.84 (m, 2H, 2′,6′-H), 7.57 (s, 1H, CH of triazole ring), 7.51–7.55 (m, 1H, 7-H), 7.36–7.41 (m, 3H, 3′,4′,5′-H), 7.32–7.35 (m, 1H, 6-H), 7.26–7.31 (m, 1H, 5-H), 5.35 (s, 2H, CH_2), 4.27 (t, J = 1.8 Hz, 2H, 2,5-C of substituted Cp ring), 4.22 (t, J = 1.8 Hz, 2H, 3,4-C of substituted Cp ring), 4.18 (s, 5H, unsubstituted Cp ring).

$^{13}C\{^1H\}$ NMR (100.62 MHz, $CDCl_3$) δ: 154.25 (7a-C), 152.26 (3-C), 140.09 (4-C of triazole ring), 130.70 (1′-C), 129.19 (6-C), 129.17 (3-C), 128.71 (2C, 3′,5′-C), 127.67 (2C, 2′,6′-C), 125.04 (4′-C), 123.35 (5-C), 121.52 (5-C of triazole ring), 121.33 (4-C), 111.14 (7-C), 107.55 (3a-C), 81.27 (1-C of substituted Cp ring), 69.15 (2C, 3,4-C of substituted Cp ring), 69.06 (5C, unsubstituted Cp ring), 68.79 (2C, 2,5-C of substituted Cp ring), 50.28 (CH_2).

FT-IR (KBr, cm^{-1}): 3090; 2930; 1454; 1439; 1059; 1038; 943; 812; 745.

MS (*m*/*z*/rel.int.): 459[M^+]/100; 395/28; 394/99; 288/17; 230/23; 207/18; 205/42; 199/23; 121/51; 56/25.

HRMS: *m*/*z* calcd for $C_{27}H_{21}FeN_3O$ $[M]^+$: 459.1034; found: 459.1028.

6b: ^{1}H NMR (400.13 MHz, $CDCl_3$) δ: 7.83–7.86 (m, 1H), 7.74–7.80 (m, 2H), 7.54 (s, 1H), 7.50–7.52 (m, 1H), 7.32–7.40 (m, 6H), 7.24–7.32 (m, 4H), 5.59 (s, 2H).

$^{13}C\{^1H\}$ NMR (100.62 MHz, $CDCl_3$) δ:154.29, 152.38, 140.75, 134.89, 130.67, 129.31 (2C), 129.23, 129.15, 128.94, 128.71 (2C), 128.07 (2C), 127.67 (2C), 125.09, 123.40, 122.02, 121.35, 111.18, 107.44, 54.40.

3.2.5. Synthesis of *N*-Ferrocenylmethyl-2-phenylbenzofuran-3-carboxamide (**7**)

The catalyst **CAT-1** (containing 1.4 μmol Pd), 3-iodo-2-phenylbenzofuran (**1**) (0.1 mmol, 32 mg), aminomethylferrocene (0.1 mmol, 21.5 mg), triethylamine (0.15 mmol, 15 mg, 20 μL) and DMF (1 mL) were placed in a stainless-steel autoclave. It was charged with carbon

monoxide (20 bar) and heated while stirring in an oil bath at 100 °C for 7 h. The catalyst was allowed to settle at room temperature and the solution was separated with a syringe. The reaction mixture was analyzed using TLC and gas chromatography. After the evaporation of the solvent, the crude product was purified using column chromatography (silica, eluent: toluene/ethyl acetate 10:1) to obtain compound 7 as a yellow solid in 61% yield.

^{1}H NMR (400.13 MHz, $CDCl_3$) δ: 7.81–8.00 (m, 3H, 4-H and 2′,6′-H), 7.42–7.56 (m, 4H, 7-H and 3′,4′,5′-H), 7.29–7.39 (m, 2H, 5,6-H), 6.05 (s, 1H, NH), 4.32 (d, J = 4.5 Hz, 2H, CH_2), 4.14–4.25 (m, 4H, 2,3,4,5-H of substituted Cp ring), 4.10 (s, 5H. unsubstituted Cp ring).

^{13}C{^{1}H} NMR (100.62 MHz, $CDCl_3$) δ: 163.47 (C=O), 154.77 (2-C), 154.01 (7a-C), 130.08 (4′-C), 129.48 (3-C), 129.03 (2C, 3′,5′-C), 128.49 (2C, 2′,6′-C), 127.84 (1′-C), 125.44 (5-C), 123.92 (6-C), 121.38 (4-C), 112.91 (3a-C), 111.35 (7-C), 84.9 (1-C of substituted Cp ring), 69.03 (5C, unsubstituted Cp ring), 68.71 (4C, 2,3,4,5-C of substituted Cp ring), 39.16 (CH_2).

FT-IR (KBr, cm^{-1}): 3395; 3281; 3081; 1634; 1511; 1454; 1440; 1258; 1201; 1099; 747.

MS (*m*/*z*/rel.int.): 435[M$^+$]/28; 249/30; 221/53; 186/29; 165/68; 164/24; 163/20; 139/21; 121/100; 78/25; 56/32; 39/24.

HRMS: *m/z* calcd for $C_{26}H_{21}FeNO_2$ [M]$^+$: 435.0922; found: 435.0919.

Side product 2-phenylbenzofuran (**8**) was characterized by GC-MS.

MS (*m*/*z*/rel.int.): 194[M$^+$]/100; 165/86; 139/21; 63/21; 39/15.

3.2.6. Synthesis of 3-Ferrocenylethynyl-2-phenylbenzofuran (**9**)

The catalyst **CAT-1** (containing 2.8 μmol Pd), CuI (2.8 μmol, 1 mg), 3-iodo-2-phenylbenzofuran (**1**) (0.1 mmol, 32 mg), ethynylferrocene (0.15 mmol, 31.5 mg), KOAc (0.2 mmol, 19.6 mg) and DMF (2 mL) were heated while stirring in an oil bath at 100 °C for 3 h. The conversion was followed by TLC and gas chromatography. The catalyst was allowed to settle at room temperature and the solution was separated with a syringe. After the evaporation of the solvent, the crude product was purified using column chromatography (silica, eluent: hexane/toluene 6:1) to obtain compound **9** as a dark orange solid: in 83% yield.

^{1}H NMR (400.13 MHz, $CDCl_3$) δ: 8.33–8.42 (m, 2H, 2′,6′-H), 7.69–7.75 (m, 1H, 4-H), 7.49–7.55 (m, 3H, 7-H and 3′,5′-H), 7.39–7.44 (m, 1H, 4′-H), 7.29–7.38 (m, 2H, 5,6-H), 4.61 (t, J = 1.8 Hz, 2H, 2,5-H of substituted Cp ring), 4.32 (t, J = 1.8 Hz, 2H, 3,4-H of substituted Cp ring), 4.31 (s, 5H, unsubstituted Cp ring).

^{13}C{^{1}H} NMR (100.62 MHz, $CDCl_3$) δ: 155.94 (2-C), 153.68 (7a-C), 130.54 (1′-C), 130.23 (3-C), 129.17 (4′-C), 128.70 (2C, 3′,5′-C), 125.96 (2C, 2′,6′-C), 125.42 (5-C), 123.45 (6-C), 120.50 (4-C), 111.30 (7-C), 100.04 (3a-C), 96.04 (≡C-Cp), 77.22 (3-C≡C), 71.72 (2C, 2,5-C of substituted Cp ring), 70.19 (5C, unsubstituted Cp ring), 69.20 (2C, 3,4-C of substituted Cp ring), 65.44 (1-C of substituted Cp ring).

FT-IR (KBr, cm^{-1}): 3094; 3019; 2214; 1454; 1441; 1123; 1063; 1024; 999; 818; 754; 689.

MS (*m*/*z*/rel.int.): 402(M$^+$)/100; 279/17; 252/21; 121/9; 56/8.

HRMS: *m/z* calcd for $C_{26}H_{18}FeO$ [M]$^+$: 402.0707; found: 402.0706

3.2.7. Synthesis of *N*-(4-((2-Phenylbenzofuran-3-yl)ethynyl)phenyl)ferrocenecarboxamide (**11**)

3-((4-Aminophenyl)ethynyl)-2-phenylbenzofuran (**10**) was synthesized based on our previous report [42].

The catalyst **CAT-1** (containing 1.4 μmol Pd), 3-((4-aminophenyl)ethynyl)-2-phenylbenzofuran (**10**) (0.2 mmol, 61.8 mg), iodoferrocene (0.1 mmol, 31.2 mg), triethylamine (0.15 mmol, 15 mg, 20 μL) and DMF (1 mL) were placed in an autoclave made of stainless steel. The reaction mixture was heated while stirring in an oil bath at 100 °C for 7 h under a carbon monoxide pressure (20 bar at room temperature). The catalyst was allowed to settle at room temperature and the solution was separated with a syringe. After the evaporation of the solvent the crude product was purified using column chromatography (silica, eluent: toluene/ethyl acetate 50:1) to obtain compound **11** as an orange solid in 98% yield.

^{1}H NMR (400.13 MHz, $CDCl_3$) δ: 8.33–8.36 (m, 2H, 2′,6′-H), 7.75–7.78 (m, 1H, 4-H), 7.61–7.68 (m, 4H, Ar^2), 7.49–7.54 (m, 3H, 7-H and 3′,5′-H), 7.45 (s, 1H, NH), 7.40–7.43 (m,

1H, 4′-H), 7.31–7.38 (m, 2H, 5,6-H), 4.86 (s, 2H, 3,4-H of substituted Cp ring), 4.50 (s, 2H, 2,5-H of substituted Cp ring), 4.33 (s, 5H, unsubstituted Cp ring).

$^{13}C\{^{1}H\}$ NMR (100.62 MHz, $CDCl_3$) δ: 168.85 (C=O), 156.34 (2-C), 153.69 (7a-C), 138.47 (4-C of Ar^2), 132.58 (2C, 2,6-C of Ar^2), 130.37 (1′-C), 130.08 (3-C), 129.29 (4′-C), 128.84 (2C, 3′,5′-C), 126.17 (2C, 2′,6′-C), 125.50 (5-C), 123.52 (6-C), 120.55 (4-C), 119.63 (2C, 3,5-C of Ar^2), 118.84 (1-C of Ar^2), 111.34 (7-C), 99.48 (3a-C), 96.77(≡C-Ar^2), 80.96 (3-C≡C), 76.23 (1-C of substituted Cp ring), 71.50 (2C, 2,5-C of substituted Cp ring), 70.31(5C, unsubstituted Cp ring), 68.67 (2C, 3,4-C of substituted Cp ring).

FT-IR (KBr, cm^{-1}): 2361; 1641; 1585; 1510; 1454; 1442; 1404; 1317, 1140; 1107; 839; 745.

3.3. Crystallography

Suitable crystals of **9** were grown by slow evaporation from $CDCl_3$. Single-crystal X-ray diffraction data were collected at 295 K on an Oxford Diffraction Gemini Ultra R diffractometer (4-circle kappa platform, Ruby CCD detector) using Mo Kα radiation. Data collection, unit cells determination and data reduction were carried out using the CrysAlis PRO [53] software package. The structures were solved with the SHELXT [54] structure solution program by Intrinsic Phasing methods and refined using full-matrix least squares on $|F|^2$ using SHELXL-2018/3 [55] with Olex2 [56] and shelXle [57] as shell. Non-hydrogen atoms were refined anisotropically. Hydrogen atoms of the ferrocene fragment were placed on calculated positions in riding mode with temperature factors fixed at 1.2 times U_{eq} of the parent carbon atoms; remaining hydrogen atoms were refined freely. The program Mercury [58] was used for molecular graphics. CCDC-2210942 entry contains the supplementary crystallographic data for this paper. These data can be obtained free of charge from The Cambridge Crystallographic Data Centre via www.ccdc.cam.ac.uk/data_request/cif (accessed on 4 October 2022).

3.4. Electrochemical Measurements

Electrochemical measurements were carried out on a BioLogic SP-150 potentiostat (reference electrode: Ag/AgCl containing 3 M KCl (in water), working electrode: glassy carbon, counter electrode: Pt-wire) using EC-LAB v.11.41 software. Cyclic voltammetric measurements were performed at room temperature under Ar in CH_2Cl_2 (2.5×10^{-3} M) with 0.1 M *n*-Bu_4NPF_6 as supporting electrolyte at a scan rate of 50 mV/s.

Diffusion coefficients were calculated for the compounds in a dichloromethane solution containing 0.1 M [*n*Bu_4N][PF_6] as an electrolyte. Sample handling and cell setup was the same as that of cyclic voltammetric measurements. Cyclic voltammograms were recorded at different polarization rates, then the peak currents were plotted as a function of the square root of polarization rate. According to the Randles-Sevcic equation, the diffusion coefficients were determined from the slope of the i_p vs. (scan rate)$^{1/2}$ plot on the basis of the following formula: $D = slope^2 \cdot \left(2.69 \times 10^5 \cdot n^{\frac{3}{2}} \cdot A \cdot c\right)^{-2}$, where D is the diffusion coefficient in $cm^2\ s^{-1}$, slope is in $AV^{-1}\ s^{-1}$, n is the change in oxidation number, A is the surface area of the working electrode in cm^2 and c is the concentration of the compound in $mol \cdot cm^{-3}$. Diffusion coefficients were determined as the mean of the individual coefficients for anodic and cathodic peaks.

For SWV experiments the samples were prepared the same way as described for the cyclic voltammetric experiments. An amount corresponding to 2.5 mM concentration of compounds **3**, **6a**, **7**, **9** and **11**, 0.1 M of [*n*Bu_4N][PF_6] and 1.25 mM of ferrocene as internal standard were dissolved in 10 mL dichloromethane, transferred into the electrochemical cell and degassed with argon bubbling. A glassy carbon electrode (previously polished using Al_2O_3 slurry) served as a working electrode, Pt wire as a counter electrode and Ag | AgCl | KCl (3 M) electrode as a reference electrode.

The potential of the working electrode, E_w was set to E_i = 0.0 V vs. ref. for 10 s, then scanning to E_v = 1.3 V vs. ref. vertex potential and back to E_f = 0.0 V vs. ref. was carried out. The pulse parameters were as follows: pulses height P_H = 25.0 mV, pulses with P_W = 50.0 ms

and a step height *SH* = 10.0 mV. Step percent was set to collect data from the rear 20% of the potential step for the average current calculation to avoid disturbances in the current signal.

The results of electrochemical experiments were analyzed using Microsoft Office Excel. A Gaussian curve fitting was carried out using the Solver target value finder plugin, ensuring that the difference between the measured and the sum of the calculated individual Gaussian curves was minimized.

3.5. Biological Activity

3.5.1. Cell Cultures

MDA-MB-231 and MCF-7 cells were purchased from ATCC (American Type Culture Collection) (Manassas, VA, USA). The cell lines were kept at 37 °C in a humified atmosphere containing 5% CO_2. MDA cells were cultured in Dulbecco's Modified Eagle's Medium Low glucose (Biosera, Nuaille, France) and completed with 10% FBS (Thermo Fisher, Life Technologies, Milan, Italy). MCF cells were cultured in Roswell Park Memorial Institute (RPMI) 1640 Medium (Biosera, Nuaille, France) and completed with 10% (*v/v*) FBS.

3.5.2. Survival Assay

To detect our treatments' effect on cell survival, we seeded MDA cells at the density of 6×10^3/well and MCF7 cells at the density of 9×10^3/well in 96-well cell culture plates for 24 h. We used our treatments at 1-10-25-50-100 μM concentrations for 24 or 48 h, after which the medium was discarded, the cells were washed with PBS (phosphate buffered saline; Biowest, Nuaille, France) and fixed in 100 μL of a cold 10% trichloroacetic acid (TCA) solution (Sigma-Aldrich Co., Budapest, Hungary). After the removal of TCA, the cells were washed with a 1% acetic acid solution (Sigma-Aldrich Co., Budapest, Hungary) and dried overnight. The following day, 70 μL 0.1% sulforhodamine B (SRB) (Sigma-Aldrich Co., Budapest, Hungary) in a 1% acetic acid solution was added to the wells for 20 min. After this, the plates were washed five times with a 1% acetic acid solution and dried for at least 2 h. We added 200 μL of a 10 mM TRIS solution (Sigma-Aldrich Co., Budapest, Hungary) to the cells and the samples were incubated at room temperature on a plate shaker for 3 h. Absorbance was measured at 560 and 600 nm simultaneously using the GloMax®-Multi Instrument (Promega, Madison, WI, USA). OD600 was subtracted as the background from the OD560 values. At least six parallel measurements were used, and the experiment was repeated three times.

4. Conclusions

Palladium-catalyzed carbonylation and Sonogashira coupling or a combination of these methodologies with copper-catalyzed azide-alkyne cycloaddition have been shown to lead to novel ferrocene-benzofuran hybrids with good to excellent yields. Besides the usual homogeneous transition metal catalysts, the reactions have also been performed with immobilized derivatives. Ferrocene-triazole-benzofuran hybrids **3** and **6a** exerted greater cytotoxic effect on MCF-7 and MDA-MB-231 than ferrocene-benzofuran hybrids **7** and **9,** proving the significant role of the triazolyl moiety in the biological effect. It is remarkable that the less curable MDA-MB-231 cell line was more sensitive to the treatments.

Supplementary Materials: The following supporting information can be downloaded at: https://www.mdpi.com/article/10.3390/inorganics10110205/s1, ^{1}H and ^{13}C NMR spectra (Figures S1–S16), results of SWV measurements (Figures S17–S21), results of biological activity tests (Figures S22–S31), crystallographic data (Table S1).

Author Contributions: Conceptualization, R.S.-F., L.K. and K.K.; methodology, E.N.; validation, K.K. and J.W.; investigation, E.N., M.V., Á.G., Z.N., K.A. and N.T.; data curation, E.N. and R.S.-F.; writing—original draft preparation, E.N. writing—review and editing, R.S.-F. and L.K.; visualization, M.V., K.A. and N.T.; supervision, R.S.-F.; funding acquisition, R.S.-F. and L.K. All authors have read and agreed to the published version of the manuscript.

Funding: The authors acknowledge the financial support of the project of the Economic Development and Innovation Operative Program of Hungary, GINOP-2.3.2-15-2016-00049 and that of the TKP2021-NKTA-21 and TKP2021-EGA-17 projects with the support provided by the Ministry of Culture and Innovation of Hungary from the National Research, Development and Innovation Fund, financed under the 2021 Thematic Excellence Programme funding scheme.

Data Availability Statement: Not applicable.

Acknowledgments: The help of Máté Fonyó in collection of the NMR data is acknowledged. We thank the PC2 technological platform of UNamur for access to the single-crystal X-ray diffractometer.

Conflicts of Interest: The authors declare no conflict of interest.

References

1. Chand, K.; Rajeshwari; Hiremathad, A.; Singh, M.; Santos, M.A.; Keri, R.S. A review on antioxidant potential of bioactive heterocycle benzofuran: Natural and synthetic derivatives. *Pharmacol. Rep.* **2017**, *69*, 281–295. [CrossRef] [PubMed]
2. Xu, Z.; Zhao, S.; Lv, Z.; Feng, L.; Wang, Y.; Zhang, F.; Bai, L.; Deng, J. Benzofuran derivatives and their anti-tubercular, anti-bacterial activities. *Eur. J. Med. Chem.* **2019**, *162*, 266–276. [CrossRef] [PubMed]
3. Xu, Z.; Xu, D.; Zhou, W.; Zhang, X. Therapeutic Potential of Naturally Occurring Benzofuran Derivatives and Hybrids of Benzofurans with other Pharmacophores as Antibacterial Agents. *Curr. Top. Med. Chem.* **2022**, *22*, 64–82. [CrossRef] [PubMed]
4. Alizadeh, M.; Jalal, M.; Khodaei Hamed, A.S.; Kheirouri, S.; Tabrizi, F.P.F.; Kamari, N. Recent updates on anti-inflammatory and antimicrobial effects of furan natural derivatives. *J. Inflamm. Res.* **2020**, *13*, 451–463. [CrossRef]
5. Farhat, J.; Alzyoud, L.; Alwahsh, M.; Al-Omari, B. Structure–activity relationship of benzofuran derivatives with potential anticancer activity. *Cancers* **2022**, *14*, 2196. [CrossRef]
6. Cabrera-Pardo, J.R.; Fuentealba, J.; Gavilán, J.; Cajas, D.; Becerra, J.; Napiórkowska, M. Exploring the multi–target neuroprotective chemical space of benzofuran scaffolds: A new strategy in drug development for Alzheimer's disease. *Front. Pharmacol.* **2020**, *10*, 1679. [CrossRef]
7. Szoke-Kovacs, Z.; More, C.; Szoke-Kovacs, R.; Mathe, E.; Frecska, E. Selective inhibition of the serotonin transporter in the treatment of depression: Sertraline, fluoxetine and citalopram. *Neuropsychopharmacol. Hung.* **2020**, *22*, 4–15.
8. Plenge, P.; Yang, D.; Salomon, K.; Laursen, L.; Kalenderoglou, I.E.; Newman, A.H.; Gouaux, E.; Coleman, J.A.; Loland, C.J. The antidepressant drug vilazodone is an allosteric inhibitor of the serotonin transporter. *Nat. Commun.* **2021**, *12*, 34417466. [CrossRef]
9. Vamos, M.; Hohnloser, S.H. Amiodarone and dronedarone: An update. *Trends Cardiovasc. Med.* **2016**, *26*, 597–602. [CrossRef]
10. Jiang, X.; Hao, X.; Jing, L.; Wu, g.; Kang, D.; Liu, X.; Zhan, P. Recent applications of click chemistry in drug discovery. *Expert Opin. Drug. Discov.* **2019**, *14*, 779–789. [CrossRef]
11. Kaur, J.; Saxena, M.; Rishi, N. An overview of recent advances in biomedical applications of click chemistry. *Bioconjugate Chem.* **2021**, *32*, 1455–1471. [CrossRef] [PubMed]
12. Gondru, R.; Kanugala, S.; Raj, S.; Kumar, C.G.; Pasupuleti, M.; Banothu, J.; Bavantula, R. 1,2,3-triazole-thiazole hybrids: Synthesis, in vitro antimicrobial activity and antibiofilm studies. *Bioorg. Med. Chem. Lett.* **2021**, *33*, 127746. [CrossRef] [PubMed]
13. Pokhodylo, N.; Shyyka, O.; Matiychuk, V. Synthesis of 1,2,3-triazole derivatives and evaluation of their anticancer activity. *Sci. Pharm.* **2013**, *81*, 663–676. [CrossRef] [PubMed]
14. Laamari, Y.; Oubella, A.; Bimoussa, A.; El Mansouri, A.E.; Ketatni, E.M.; Mentre, O.; Auhmani, A. Design, hemiysnthesis, crystal structure and anticancer activity of 1, 2, 3-triazoles derivatives of totarol. *Bioorg. Chem.* **2021**, *115*, 105165. [CrossRef]
15. Ren, Y.; Liu, Y.; Gao, S.; Dong, X.; Xiao, T.; Jiang, Y. Palladium-catalyzed selective ortho C–H alkoxylation at 4-aryl of 1, 4-disubstituted 1, 2, 3-triazoles. *Tetrahedron* **2020**, *76*, 130985. [CrossRef]
16. Kant, R.; Kumar, D.; Agarwal, D.; Gupta, R.D.; Tilak, R.; Awasthi, S.K.; Agarwal, A. Synthesis of newer 1,2,3-triazole linked chalcone and flavone hybrid compounds and evaluation of their antimicrobial and cytotoxic activities. *Eur. J. Med. Chem.* **2016**, *113*, 34–49. [CrossRef]
17. Sun, L.; Huang, T.; Dick, A.; Meuser, M.E.; Zalloum, W.A.; Chen, C.H.; Liu, X. Design, synthesis and structure-activity relationships of 4-phenyl-1H-1, 2, 3-triazole phenylalanine derivatives as novel HIV-1 capsid inhibitors with promising antiviral activities. *Eur. J. Med. Chem.* **2020**, *190*, 112085. [CrossRef]
18. Battigelli, A.; Almeida, B.; Shukla, A. Recent Advances in Bioorthogonal Click Chemistry for Biomedical Applications. *Bioconjugate Chem.* **2022**, *33*, 263–271. [CrossRef]
19. Sodhi, R.K.; Paul, S. Metal Complexes in medicine: An overview and update from drug design perspective. *Cancer Ther. Oncol. Int. J.* **2019**, *14*, 25–32. [CrossRef]
20. Chellan, P.; Sadler, P.J. Enhancing the Activity of drugs by conjugation to organometallic fragments. *Chem. Eur. J.* **2020**, *26*, 8676–8688. [CrossRef]
21. Yousuf, I.; Bashir, M.; Arjmand, F.; Tabassum, S. Advancement of metal compounds as therapeutic and diagnostic metallodrugs: Current frontiers and future perspectives. *Coord. Chem. Rev.* **2021**, *445*, 214104. [CrossRef]
22. Patra, M.; Gasser, G. The medicinal chemistry of ferrocene and its derivatives. *Nat. Rev. Chem.* **2017**, *1*, 0066. [CrossRef]

23. Singh, A.; Lumb, I.; Mehra, V.; Kumar, V. Ferrocene-appended pharmacophores: An exciting approach for modulating biological potential of organic scaffolds. *Dalton Trans.* **2019**, *48*, 2840–2860. [CrossRef]
24. Top, S.; Tang, J.; Vessieres, A.; Carrez, D.; Provot, C.; Jaouen, G. Ferrocenyl hydroxytamoxifen: A prototype for a new range of oestradiol receptor site-directed cytotoxics. *Chem. Commun.* **1996**, *8*, 955–956. [CrossRef]
25. McCarthy, J.S.; Rückle, T.; Djeriou, E.; Cantalloube, C.; Ter-Minassian, D.; Baker, M.; O'Rourke, P.; Griffin, P.; Marquart, L.; van Huijsduijnen, R.H.; et al. A Phase II pilot trial to evaluate safety and efficacy of ferroquine against early Plasmodium falciparum in an induced blood-stage malaria infection study. *Malar. J.* **2016**, *15*, 469. [CrossRef] [PubMed]
26. Torres, J.C.; Pilli, R.A.; Vargas, M.D.; Violante, F.A.; Garden, S.J.; Pinto, A.C. Synthesis of 1-ferrocenyl-2-aryl (heteroaryl) acetylenes and 2-ferrocenylindole derivatives via the Sonogashira–Heck–Cassar reaction. *Tetrahedron* **2002**, *58*, 4487–4492. [CrossRef]
27. Zhao, C.; Liu, Z.Q. Modification by ferrocene: An approach to enhance antioxidant ability of ailanthoidol to protect DNA. *Biochimie* **2012**, *94*, 1805–1811. [CrossRef] [PubMed]
28. Franz, K.J. Application of inorganic chemistry for non-cancer therapeutics. *Dalton Trans.* **2012**, *41*, 6333–6334. [CrossRef]
29. Zhuoma, B.; Li, Y.; Gao, W. First synthesis of 2-ferrocenoyl-3-methylbenzofuran derivatives. *J. Chem. Res.* **2015**, *39*, 82–85. [CrossRef]
30. Li, Y.; Zhuoma, B.; Gao, W. A Novel synthesis of 2-ferrocenoyl-substituted iodobenzofurans. *J. Heterocycl. Chem.* **2017**, *54*, 764–768. [CrossRef]
31. Liang, Z.; Xu, H.; Tian, Y.; Guo, M.; Su, X.; Guo, C. Design, synthesis and antifungal activity of novel benzofuran-triazole hybrids. *Molecules* **2016**, *21*, 732. [CrossRef] [PubMed]
32. Sunitha, V.; Kishore Kumar, A.; Shankar, B.; Anil Kumar, A.; Krishna, T.M.; Lincoln, C.A.; Pochampalli, J. Synthesis and antimicrobial activity of some novel benzofuran based 1, 2, 3-triazoles. *Russ. J. Gen. Chem.* **2017**, *87*, 322–330. [CrossRef]
33. Qi, Z.Y.; Hao, S.Y.; Tian, H.Z.; Bian, H.L.; Hui, L.; Chen, S.W. Synthesis and biological evaluation of 1-(benzofuran-3-yl)-4-(3, 4, 5-trimethoxyphenyl)-1H-1,2,3-triazole derivatives as tubulin polymerization inhibitors. *Bioorg. Chem.* **2020**, *94*, 103392. [CrossRef] [PubMed]
34. Urbán, B.; Papp, M.; Skoda-Földes, R. Carbonylation of aryl halides in the presence of heterogeneous catalysts. *Curr. Green Chem.* **2019**, *6*, 78–95. [CrossRef]
35. McCarthy, S.; Braddock, D.C.; Wilton-Ely, J.D.E.T. Strategies for sustainable palladium catalysis. *Coord. Chem. Rev.* **2021**, *442*, 213925. [CrossRef]
36. Mandoli, A. Recent advances in recoverable systems for the copper-catalyzed azide-alkyne cycloaddition reaction (CuAAC). *Molecules* **2016**, *21*, 1174. [CrossRef]
37. Neumann, S.; Biewend, M.; Rana, S.; Binder, W.H. The CuAAC: Principles, homogeneous and heterogeneous catalysts, and novel developments and applications. *Macromol. Rapid Commun.* **2020**, *41*, 1900359. [CrossRef]
38. López, O.; Padrón, J.M. Iridium- and palladium-based catalysts in the pharmaceutical industry. *Catalysts* **2022**, *12*, 164. [CrossRef]
39. Rani, A.; Singh, G.; Singh, A.; Maqbool, U.; Kaur, G.; Singh, J. CuAAC-ensembled 1,2,3-triazole-linked isosteres as pharmacophores in drug discovery: Review. *RSC Adv.* **2020**, *10*, 5610–5635. [CrossRef]
40. Alonso, D.A.; Baeza, A.; Chinchilla, R.; Gómez, C.; Guillena, G.; Pastor, I.M.; Ramón, D.J. Solid-supported palladium catalysts in Sonogashira reactions: Recent developments. *Catalysts* **2018**, *8*, 202. [CrossRef]
41. Adamcsik, B.; Nagy, E.; Urbán, B.; Szabó, P.; Skoda-Földes, R. Palladium nanoparticles on a pyridinium supported ionic liquid phase: A recyclable and low-leaching palladium catalyst for aminocarbonylation reactions. *RSC Adv.* **2020**, *10*, 23988–23998. [CrossRef] [PubMed]
42. Nagy, E.; Nagymihály, Z.; Kollár, L.; Fonyó, M.; Skoda-Földes, R. Synthesis of 3-aryl- and 3-alkynyl benzofurans in the presence of a supported palladium catalyst. *Synthesis* **2022**. [CrossRef]
43. Fehér, K.; Nagy, E.; Szabó, P.; Juzsakova, T.; Srankó, D.; Gömöry, Á.; Kollár, L.; Skoda-Földes, R. Heterogeneous azide–alkyne cycloaddition in the presence of a copper catalyst supported on an ionic liquid polymer/silica hybrid material. *Appl. Organomet. Chem.* **2018**, *32*, e4343. [CrossRef]
44. Fehér, K.; Balogh, J.; Csók, Z.; Kégl, T.; Kollár, L.; Skoda-Földes, R. Synthesis of ferrocene-labeled steroids via copper-catalyzed azide–alkyne cycloaddition. Reactivity difference between 2β-, 6β- and 16β-azido-androstanes. *Steroids* **2012**, *77*, 738–744. [CrossRef]
45. Lasányi, D.; Mészáros, Á.; Novák, Z.; Tolnai, G.L. Catalytic Activation of trimethylsilylacetylenes: A one-pot route to unsymmetrical acetylenes and heterocycles. *J. Org. Chem.* **2018**, *83*, 8281–8291. [CrossRef]
46. Shultz, D.A.; Gwaltney, K.P.; Lee, H. A modified procedure for Sonogashira couplings: Synthesis and characterization of a bisporphyrin, 1,1-bis[zinc(II)5′-ethynyl-10′,15′,20′-trimesitylporphyrinyl]methylenecyclohexane. *J. Org. Chem.* **1998**, *63*, 4034–4038. [CrossRef]
47. Friscourt, F.; Boons, G.J. One-pot three-step synthesis of 1, 2, 3-triazoles by copper-catalyzed cycloaddition of azides with alkynes formed by a Sonogashira cross-coupling and desilylation. *Org. Lett.* **2010**, *12*, 4936–4939. [CrossRef]
48. Cuevas, F.; Oliva, A.I.; Pericas, M.A. Direct copper (I)-catalyzed cycloaddition of organic azides with TMS-protected alkynes. *Synlett* **2010**, *2010*, 1873–1877. [CrossRef]
49. Stefani, H.A.; Amaral, M.F.; Manarin, F.; Ando, R.A.; Silva, N.C.; Juaristi, E. Functionalization of 2-(S)-isopropyl-5-iodo-pyrimidin-4-ones through Cu (I)-mediated 1, 3-dipolar azide–alkyne cycloadditions. *Tetrahedron Lett.* **2011**, *52*, 6883–6886. [CrossRef]

50. Carmona-Negrón, J.A.; Santana, A.; Rheingold, A.L.; Meléndez, E. Synthesis, structure, docking and cytotoxic studies of ferrocene–hormone conjugates for hormone dependent breast cancer application. *Dalton Trans.* **2019**, *48*, 5952–5964. [CrossRef]
51. Casas-Solvas, J.M.; Vargas-Berenguel, A.; Capitán-Vallvey, L.F.; Santoyo-González, F. Convenient methods for the synthesis of ferrocene–carbohydrate conjugates. *Org. Lett.* **2004**, *6*, 3687–3690. [CrossRef] [PubMed]
52. Lin, W.; Zhang, X.; He, Z.; Jin, Y.; Gong, L.; Mi, A. Reduction of azides to amines or amides with zinc and ammonium chloride as reducing agent. *Synth. Commun.* **2002**, *32*, 3279–3284. [CrossRef]
53. Rigaku Oxford Diffraction. *CrysAlis PRO*; Version 1.171.40.67a; Rigaku Oxford Diffraction Ltd.: Yarnton, UK, 2019.
54. Sheldrick, G.M. SHELXT—Integrated space-group and crystal-structure determination. *Acta Crystallogr. Sect. A Found. Crystallogr.* **2015**, *71*, 3–8. [CrossRef] [PubMed]
55. Dolomanov, O.V.; Bourhis, L.J.; Gildea, R.J.; Howard, J.A.K.; Puschmann, H.J. OLEX2: A complete structure solution, refinement and analysis program. *Appl. Crystallogr.* **2009**, *42*, 339–341. [CrossRef]
56. Sheldrick, G.M. Crystal structure refinement with SHELXL. *Acta Crystallogr. Sect. C Struct. Chem.* **2015**, *71*, 3–8. [CrossRef] [PubMed]
57. Hübschle, C.B.; Sheldrick, G.M.; Dittrich, B.J. ShelXle: A Qt graphical user interface for SHELXL. *Appl. Crystallogr.* **2011**, *44*, 1281–1284. [CrossRef]
58. Macrae, C.F.; Sovago, I.; Cottrell, S.J.; Galek, P.T.A.; McCabe, P.; Pidcock, E.; Platings, M.; Shields, G.P.; Stevens, J.S.; Towler, M.; et al. Mercury 4.0: From visualization to analysis, design and prediction. *J. Appl. Crystallogr.* **2020**, *53*, 226–235. [CrossRef]